

Numerical study three-dimensional of mixed convection in a cavity: Influence of Reynolds and Grashof numbers

Open
Access

Razik Benderradji^{1,2,*}, Hamza Goudmi², Djedid Taloub^{1,2}, Abdelhadi Beghidja²

¹ Department of Physics, Faculty of Science, University Med Boudiaf M'sila, Algeria

² Laboratory of Renewable Energy and Sustainable Development (LREDD), University of the Mentouri Brothers, Constantine 1, Algeria

ARTICLE INFO

ABSTRACT

Article history:

Received 20 July 2018

Received in revised form 12 August 2018

Accepted 1 November 2018

Available online 6 November 2018

Keywords:

mixed convection, cavity, multi clear structure, number of Grashof and Reynolds

In this work, we present a numerical study of mixed convection heat exchange in a cubic cavity of a laminar three-dimensional (3D) incompressible flow. This study predicted the behavior of the flow structure between Multi clear structure dominated by natural convection when the Reynolds number is small, and a Multi clear structure dominated by forced convection when the Reynolds number is high. First, we fix the Grashof number for the variable Reynolds number. Second, we vary the number of Grashof for which the Reynolds number is kept fixed. The results obtained give a clear comparison with those found in the literature it examines and explains the thermal and dynamic characteristics of the flow.

Copyright © 2018 PENERBIT AKADEMIA BARU - All rights reserved

1. Introduction

For many years, laminar and turbulent flows of closed cavity natural convection have been the subject of numerous numerical and experimental studies, such as the work of Ogut [1], Baracoset *al.*, [2], Dixit *et al.*, [3], Saati *et al.*, [4], and those of mixed convection such as the work of Haigermoser *et al.*, [5], Med Tofiqui Islam *et al.* [6], SumonSaha *et al.*, [7], Krishnakumaret *al.*, [8], Rahman *et al.*, [9], Bouaraouret *al.*, [10]. They studied rectangular cavities. On the one hand these studies were carried out under conditions where the Reynolds number is varied and on the other hand, it is constant. It is the same for the number of Grashof but in the opposite direction. The interest in this type of flow comes from the fact that, for many industrial applications, in particular, the compressor (and the turbine (rotor-stator), the analysis of the phenomena involves forces of stability thrusts which, coupling with a confining effect, give rise to complex and varied flows. This complexity is accentuated by the generally unsteady character. All these motions of the fluids motivated fundamental studies aiming to better apprehend the couplings between the dynamics and the thermal of such systems, the interactions between the moving fluid and the walls, the influence of the geometry or the boundary conditions (with imposed temperature conditions or imposed heat fluxes), the appearance and development of vortex instabilities. Turbulence is generally described as a disordered flow in time and space. It is unpredictable in the sense that a small initial disturbance at a given instant

amplifies rapidly and makes a deterministic prediction of its evolution impossible. It presents structures in motion that are organized and identifiable (coherent structures) or perfectly disordered, thus helping to amplify the transfer and reinforce mixing mechanisms. As is the case of the rectangular cavity of the sidewalls heated with a horizontal flow that flows at a constant speed, Doghmimet *al.*, [12], Md. Shah Jaman *et al.*, [13], and Antonio Carozza [14]. For this reason, the phenomenon of mixed convection and the study of the structure of the flow at the level of the cavity are treated. This study is therefore based on two aspects:

- In the first one, the Grashof number is fixed and the Reynolds number is varied to study the effect of acceleration of flow on behavior and structure.
- The last case presents the effect of Grashof number to show the effect of the buoyancy forces on the iso-line of temperature and the appearance of the eddies. This explains the criterion of instability. The lines of the isotherms and the current functions are presented to give greater clarity to this phenomenon.

2. Geometry and Simulation Methods

The problem is to study the flow of air in a cubic 3D cavity. A schematic representation of the geometrical configuration studied is shown in Figure 1. This cavity is subjected to an external flow entering the lower part of the left vertical wall with a speed u_1 and a temperature T_1 . The acceleration of gravity acts parallel to the side walls. The wall on the right with respect to the horizontal, in the direction X , is maintained at a hot temperature T_c . And the left one and the other walls are kept adiabatic.

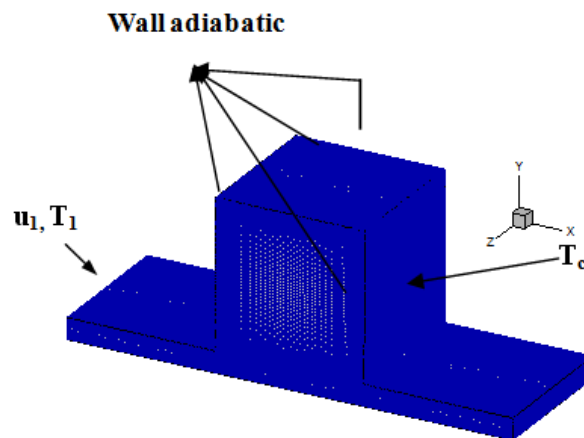


Fig. 1. Diagram of the domain of calculation

Matet *al.*, [7] has performed a comprehensive flow visualization studies on blunt-edge delta wing. The primary vortex is developed at certain chordwise position and progress upstream with angle of attack. However, there is no data in VFE-2 indicating that the vortex progressed up to the Apex region with angle of attack increases.

3. Mathematical Model

3.1 Equations Governing

The flow is considered to be three-dimensional, stationary and laminar, and the physical properties are assumed to be constant except for the density in the expression of the buoyancy force of the motion equation in the vertical direction, using the Boussinesq approximation. Viscous dissipation in the energy equation is neglected. The working fluid is assumed to be air ($Pr = 0.71$). Considering the assumptions mentioned above, the governing equations can be written in three-dimensional form as follows.

Continuity equation.

$$\frac{\partial U}{\partial X} + \frac{\partial V}{\partial Y} + \frac{\partial W}{\partial Z} = 0 \quad (1)$$

Equation of moment on x.

$$U \frac{\partial U}{\partial X} + V \frac{\partial U}{\partial Y} + W \frac{\partial U}{\partial Z} = -\frac{\partial P}{\partial X} + \frac{1}{Re} \left(\frac{\partial^2 U}{\partial X^2} + \frac{\partial^2 U}{\partial Y^2} + \frac{\partial^2 U}{\partial Z^2} \right) \quad (2)$$

Equation of moment on y.

$$U \frac{\partial V}{\partial X} + V \frac{\partial V}{\partial Y} + W \frac{\partial V}{\partial Z} = -\frac{\partial P}{\partial Y} + \frac{1}{RePr} \left(\frac{\partial^2 V}{\partial X^2} + \frac{\partial^2 V}{\partial Y^2} + \frac{\partial^2 V}{\partial Z^2} \right) + \frac{Gr}{Re^2} \theta \quad (3)$$

Equation of moment on z.

$$U \frac{\partial W}{\partial X} + V \frac{\partial W}{\partial Y} + W \frac{\partial W}{\partial Z} = -\frac{\partial P}{\partial Z} + \frac{1}{Re} \left(\frac{\partial^2 W}{\partial X^2} + \frac{\partial^2 W}{\partial Y^2} + \frac{\partial^2 W}{\partial Z^2} \right) \quad (4)$$

Equation of energy.

$$U \frac{\partial \theta}{\partial X} + V \frac{\partial \theta}{\partial Y} + W \frac{\partial \theta}{\partial Z} = \frac{1}{RePr} \left(\frac{\partial^2 \theta}{\partial X^2} + \frac{\partial^2 \theta}{\partial Y^2} + \frac{\partial^2 \theta}{\partial Z^2} \right) \quad (5)$$

The mixed convection parameter seen in the above equation, Gr/Re^2 , is also called the Richardson number, Ri . Note that the Grashof number is based on the temperature difference of the hot side walls and fluid because the type of boundary conditions is considered as the heating element to the walls. The dimensionless numbers observed in the above equations, Re , Gr , and Pr , are respectively the numbers of Reynolds, Grashof, and Prandtl. They are defined as follows.

$$Re = \frac{u_1 H}{\nu}, \quad Gr = \frac{g \beta \Delta T H^3}{\nu^2}, \quad Pr = \frac{\nu}{\alpha} \quad (6)$$

The dimensionless parameters in the equations above are defined as follows.

$$X = \frac{x}{H}, \quad Y = \frac{y}{H}, \quad Z = \frac{z}{H}, \quad U = \frac{u}{u_1}, \quad V = \frac{v}{u_1}, \quad W = \frac{w}{u_1}, \quad P = \frac{p}{\rho u_1^2}, \quad \theta = \frac{T - T_1}{T_C - T_1} \quad (7)$$

3.2 Boundary Conditions

The boundary conditions used in this study are given in dimensionless form as follows.

On the side walls.

$$U=V=W=0, \theta=1 \quad (8)$$

The rest of the walls.

$$U=V=W=0, \partial\theta/\partial Y=0 \quad (9)$$

At the exit of the cavity.

$$V = \partial\theta/\partial X = \partial U/\partial X = \partial W/\partial X = 0 \quad (10)$$

At the entrance of the cavity.

$$V = W = \theta = 0, U = 1 \quad (11)$$

In order to compare the total heat flux, we use the local and average Nusselt number which is defined as follows.

$$Nu_y = \frac{\left(\frac{\partial\theta}{\partial y}\right)_{Y=1}}{\theta_C - \theta_1}, \quad Nu_H = \int_1^8 Nu_y dY \quad (12)$$

3.3 Numerical Algorithms

The coupled governing equations are transformed into sets of algebraic equations using the finite volume method and are solved by the SIMPLE algorithm [11]. The offset grid system is used, and the convective terms are processed by the second order centered Upwind scheme. The mesh adopted in this study is a non-uniform mesh in both directions (horizontal and vertical) and characterized by 6726 nodes. It is finer near the walls where a significant change in physical variables is expected.

4. Analysis and Interpretation of Results

The results present two cases. The first is performed for different values of the Reynolds number, $Re = 10, 50, 100, 500, 1000$ and 2000 . The second case varies the Grashof number in the range of (10^3) , up to 10^6 .

Case 1, influence of the Reynolds number. The structure of the flow, the thermal field, and the heat transfer through the hot wall are examined in this section for different Reynolds number values ($Re = 10$ to 2000), to see the effect on the structure of flow and heat transfer, in this case the Prandtl number is constant, 0.74 and the Grashof number equal to 10^3 . The isotherms are shown in Figure 2. On median planes (oxy), (oyz), (oxz) respectively. The distribution of the heat in the cavity conforms to the circulation of the fluid revealed by the iso-current lines illustrated in Figure 3. Indeed, we observe a heating of the fluid along the right wall closer to the heating element to the output for all values of the Reynolds number. It will be noted that, in the vicinity of the hot wall and the other cold walls, the existence of a crushing of the fluid due to the reduction of the passage cross-section at the inlet of the cavity, we find that the isotherms are almost Parallels for low Reynolds values.

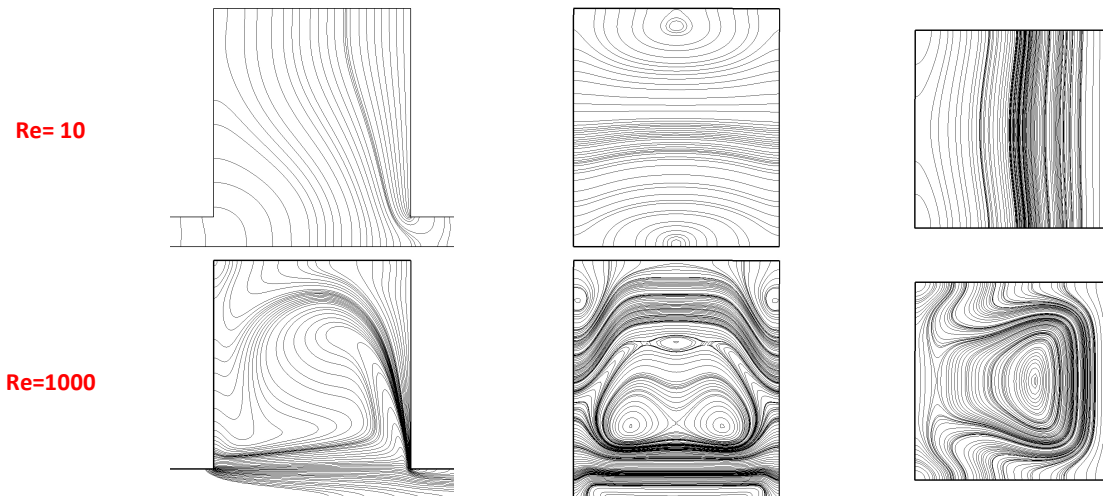


Fig. 2. Isotherms for different Reynolds numbers, on median planes (oxy), (oyz), (oxz)

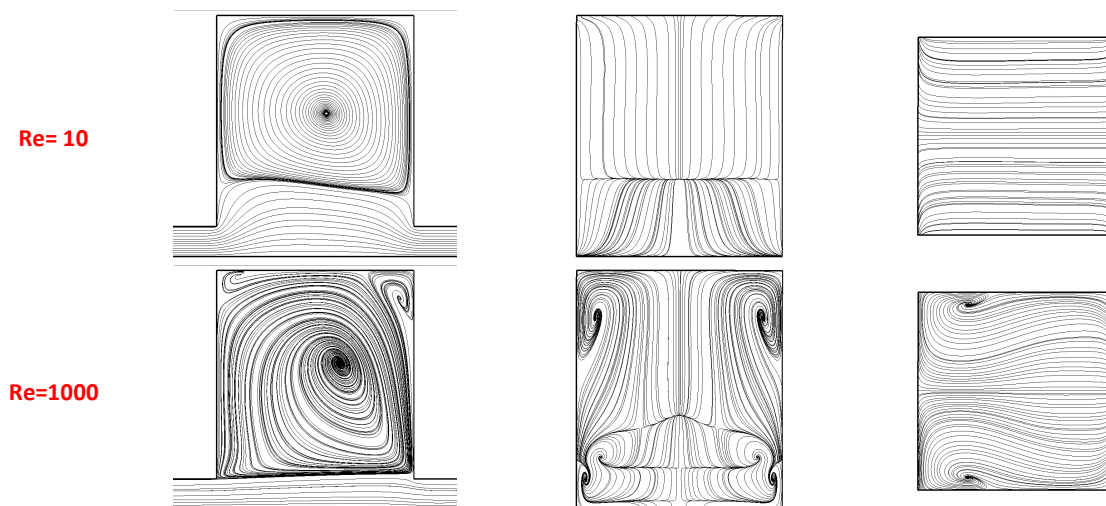


Fig. 3. Iso lines of currents for different Reynolds number, on median planes (oxy), (oyz), (oxz)

The position of the heating element influences the heat transfer, it is noted that the high temperatures are located in narrow spaces in the vicinity of the hot wall, which correspond to the thickness of the thermal boundary layers and which are largely influenced by the number of Reynolds. Far from the hot wall, the temperature gradients are low. A different flow structure is observed for each Reynolds number which makes it possible to detect the presence of the main vortex and/or the secondary vortices for increasingly large numbers. Note also for example for $Re = 10$, and $Re = 50$, symmetrical cell is translated by the function Q (iso-temperature surfaces within the cubic cavity), illustrated in Figure 4. It explains the predominance of natural convection. When the Reynolds number increases, vortex instability is marked by the flow jet effect, which changes the nature of heat transfer by natural convection to forced convection and the main cell is positioned at the center of the cavity.

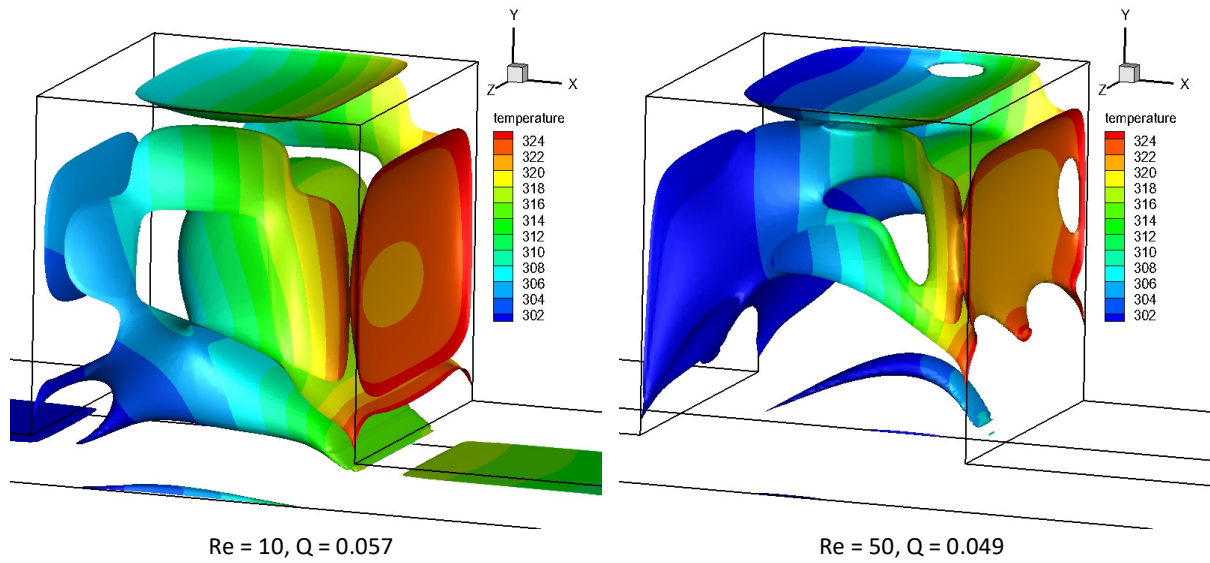


Fig. 4. Iso temperature surfaces

Figure 5 and Figure 6 demonstrate the evolution of temperature and the profile of the vertical velocity of the cavity on the horizontal line $X = 0.035$, for the different Reynolds number values, as seen in Figure 5. Temperature increases with increasing altitude, just after position $Y = 0.01$. The figure is composed of two distinct zones, from $Y = 0$ to $Y = 0.01$. The temperature increases with the increase of the altitude and remain almost constant than just after the position $Y = 0.01$. Increases substantially, up to the value of the hot wall (T_c). Furthermore, it is also shown that the improvement in the generation of entropy and heat transfer increases considerably with increasing Reynolds number.

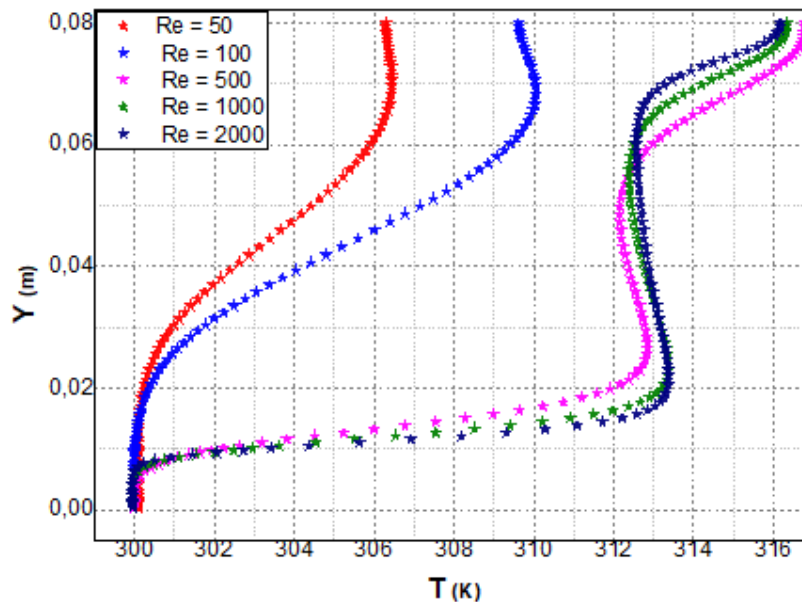


Fig. 5. Horizontal temperature profiles at $X = 0.035$ for different Reynolds numbers

The profile of the half-length velocity of the cavity for the different Reynolds numbers chosen is shown in Figure 6. It is noted that the maxima are proportional to the Reynolds number and that its

positions are closer to the wall Warm when actually increasing the Reynolds number. This is due to the combined effects of jet convection and thermal thrust in the horizontal direction where the boundary layers become thick with the intensification of the flow. However, maximum velocity values are encountered in the range $0.0 < X < 0.6$. These values indicate where the flowing particles follow the moving current lines.

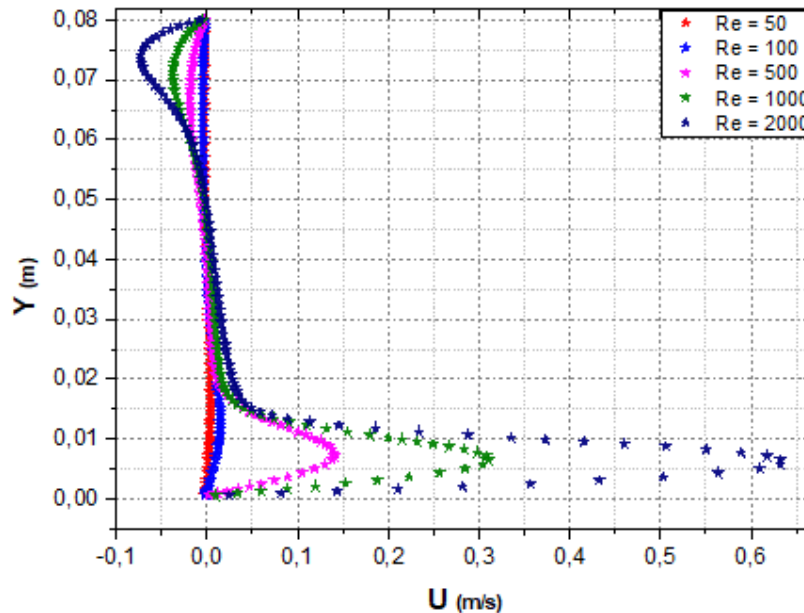


Fig. 6. Horizontal velocity profiles at $X = 0.035$ for different Reynolds numbers

Case 2, influence of the number of Grashof. In natural convection the Rayleigh number is the important parameter that determines the nature of the thermal flow. It represents the ratio of buoyancy forces (Archimedes' forces) to viscous forces. It is proportional to the applied temperature gradient. The flow is characterized by the movement of fluid due to the hot side wall of the cavity. When the Reynolds number is taken, $Re = 200$, as constant, and the Grashof number ($Gr = 10^3$ to 10^6) is varied, the current functions as well as the isothermal distributions are shown in Figure 7, and Figure 8.

Note that when the number of Grashof increases progressively the vortex structure is more and more deformed thus giving an elliptic shape. In addition, it is also noted that for $10^4 \leq Gr \leq 10^6$ the current lines are almost parallel along the vertical plane with a symmetrical configuration which is illustrated in Figure 9. From the function Q , the isotherms of the flow are shown in Figure 8. It is noted that the high temperatures are located in narrow spaces in the vicinity of the hot wall, which correspond to the thickness of the thermal boundary layers and which are largely influenced by the number Of Richardson.

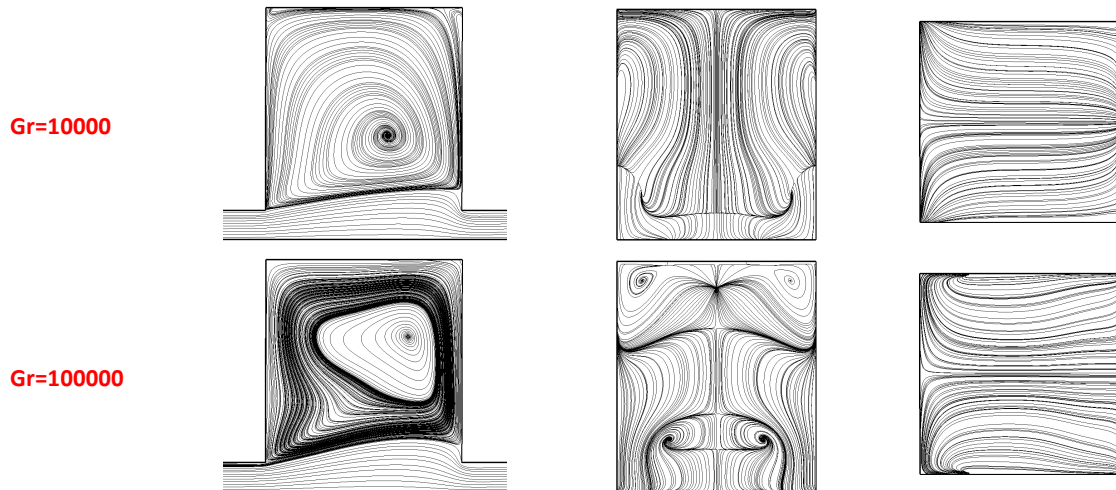


Fig. 7. Iso lines of currents for different Grashof number, on median planes (oxy), (oyz), (oxz)

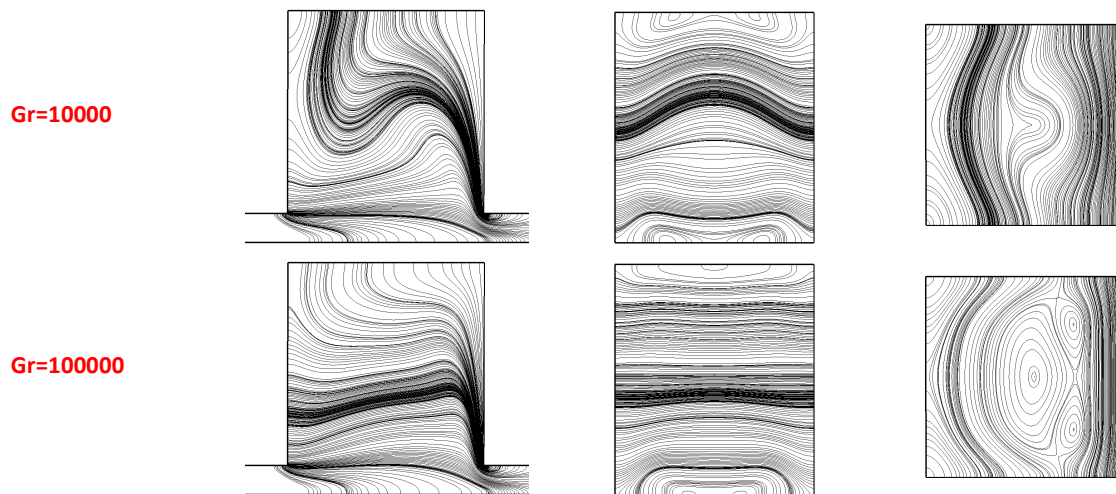


Fig. 8. Isotherms for different Grashof numbers, on median planes (oxy), (oyz), (oxz)

Away from the hot walls, the temperature gradients are low. There is also no thermal stratification in the cavity for $10^3 \leq Gr \leq 10^4$. Thermal stratification begins to appear in the middle of the cavity only from $Gr = 10^4$ where natural convection is dominant. This stratification is increasingly developed towards the area which lies above the lower extremities of the heated side walls. The heat recovered from the hot wall is carried by convection downwards and in the middle of the enclosure. By increasing the number of Grashof the isotherms in the center of the enclosure become wider and less stratified, this is due to the dominance of the buoyancy forces with respect to shear forces for more justification regarding the temperature distribution in the cavity. Figure 10 shows the temperature profiles, at $X = 0.035$, where we find minimal values at the bottom of the cavity increased with the Richardson number increase.

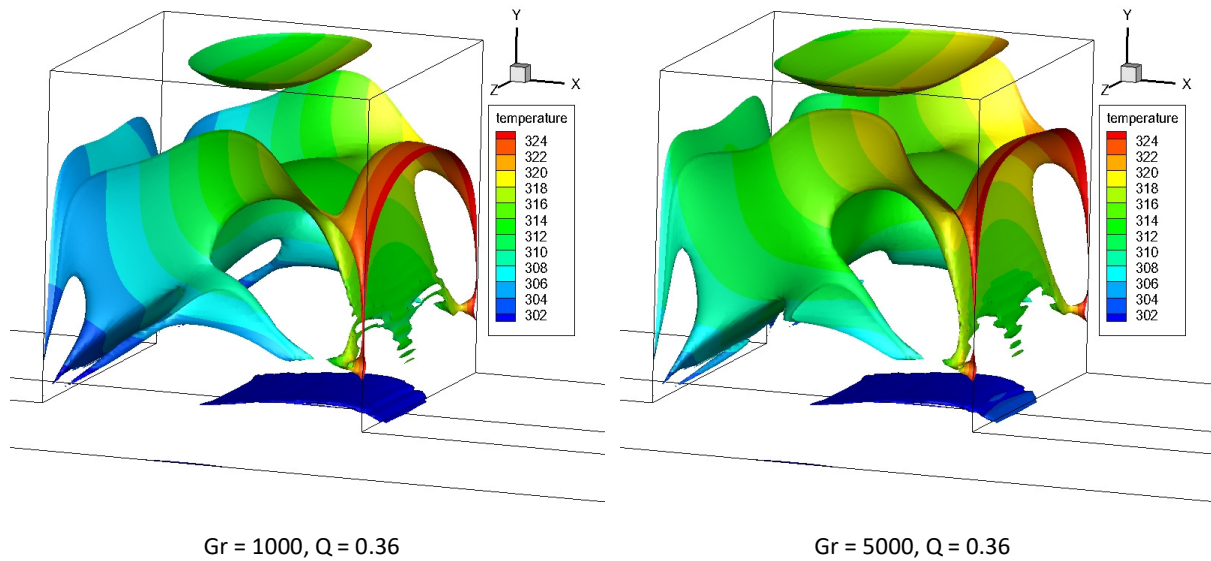


Fig. 9. Iso temperature surfaces

The graph in Figure 11, which shows the profile of the velocity U along $X = 0.035$, shows the increase in the horizontal velocity in both directions with respect to the upper deviation point for Grashof numbers greater than 1000.

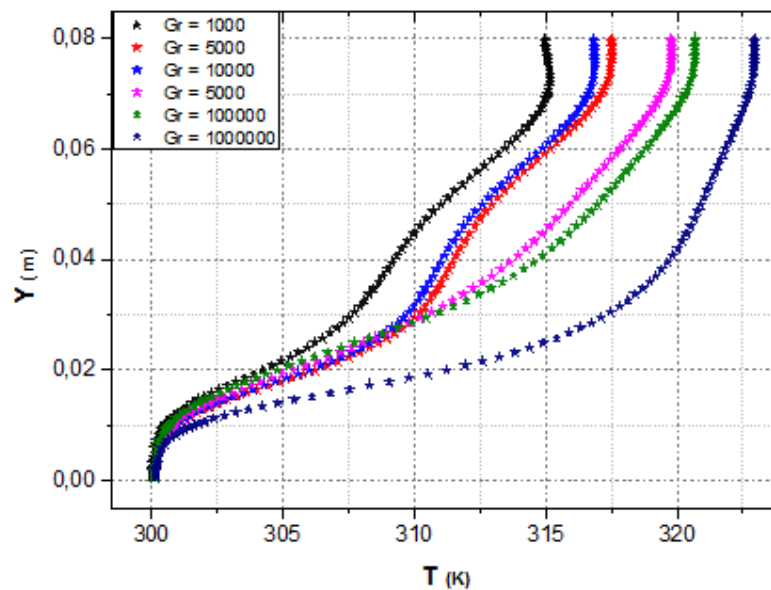


Fig. 10. Horizontal temperature profiles at $X = 0.035$ for different Reynolds numbers

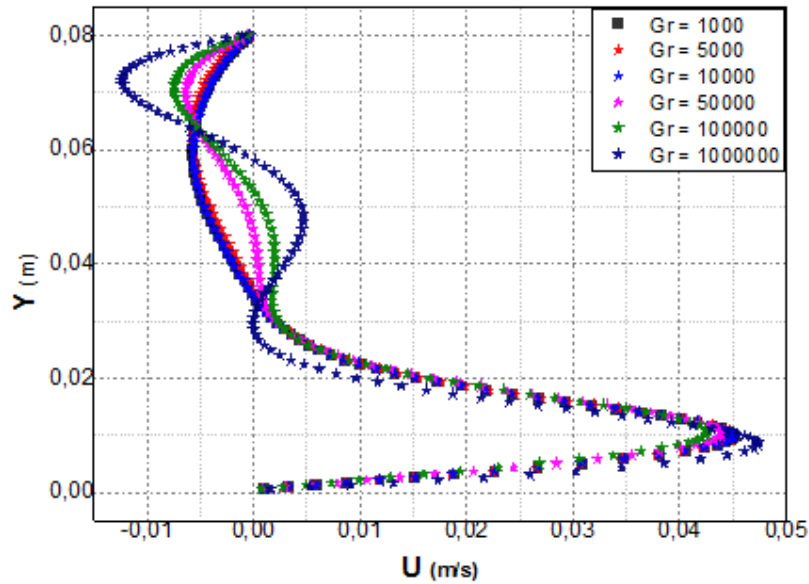


Fig. 11. Horizontal velocity profiles at $X = 0.035$ for different Reynolds numbers

The heat transfer allows the local and middle Nusselt numbers to be plotted at the hot sidewall level. The variation in the number of the mean Nusselt in relation to the Reynolds number is shown in Figure 12. The Reynolds number effect on the Nusselt number is translated according to a power law of the type $Nu = a Re^b$ as consider. As the number of Reynolds increases, the number of Nusselt also gradually increases over the entire parts heap. The maximum value of the Nusselt number is obtained for the highest value of Re . We also find that the intensity of the heat transfer increases with the increase of the Reynolds number, near the heated part. This is due to the dominance of buoyancy forces.

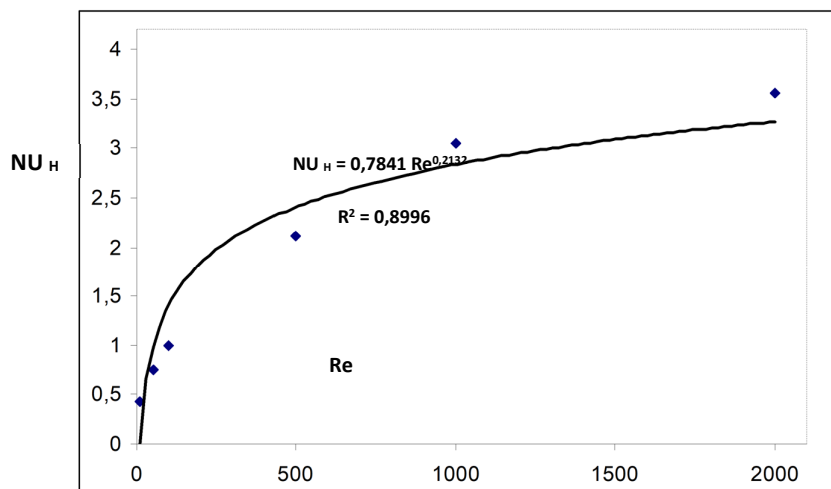


Fig. 12. Variation of the mean Nusselt number as a function of the Reynolds number

5. Conclusions

In this work we have presented a numerical approach to laminar mixed convection that develops in a cubic cavity under the Boussinesq hypothesis. The study was conducted according to Grashof number and Reynolds number. The finite volume method has been adopted for the resolution of the resulting algebraic system. It presents, examines and explains the thermal and dynamic characteristics of the flow for two aspects: The first is to set the Grashof number to 10^3 , and the Reynolds number is varied. The second is devoted to the variation of the number of Grashof and to keep the Reynolds number at 200, as constant.

The numerical results obtained show a Multi clear structure stationary flow regime whose size and shape of the cells depend strongly on the Grashof number and the Reynolds number. The variation of the heat transfer is expressed by the number of the mean Nusselt in the form of the power law of type $Nu = c Gr^d$.

References

- [1] Buuml, Elif. "Mixed convection in an inclined lid-driven enclosure with a constant flux heater using differential quadrature (dq) method." *International Journal of Physical Sciences* 5, no. 15 (2010): 2287-2303.
- [2] Barakos, G., Ee Mitsoulis, and Do Assimacopoulos. "Natural convection flow in a square cavity revisited: laminar and turbulent models with wall functions." *International Journal for Numerical Methods in Fluids* 18, no. 7 (1994): 695-719.
- [3] Dixit, H. N., and V. Babu. "Simulation of high Rayleigh number natural convection in a square cavity using the lattice Boltzmann method." *International journal of heat and mass transfer* 49, no. 3-4 (2006): 727-739.
- [4] Saati, A. A., Bawazeer. S. A, "The natural convection in cavities with a Thin Fin on the hot wall using the lattice Boltzmann method," In *Proceedings of ICFD 10: then international congress of fluid dynamics*, Stella Di Mare Sea Club Hotel, Ain Soukhna, Red Sea, Egypt, 2010.
- [5] Haigermoser, Christian, F. Scarano, Michele Onorato, P. Torino, and T. Delft. "Investigation of the flow in a rectangular cavity using tomographic and time resolved PIV." In *Proceedings of ICAS 26th International Congress of the Aeronautical Sciences, Anchorage, AK*. 2008.
- [6] Islam, Md Tofiqul, Sumon Saha, Md Arif Hasan Mamun, and Mohammad Ali. "Two dimensional numerical simulation of mixed convection in a rectangular open enclosure." *Fluid Dyn. Mater. Process* 4, no. 2 (2008): 125-138.
- [7] Saha, Sumon, Md Tofiqul Islam, Mohammad Ali, Md Arif Hassan Mamun, and M. Quamrul Islam. "Effect of inlet and outlet locations on transverse mixed convection inside a vented enclosure." *Journal of Mechanical Engineering* 36 (2006): 27-37.
- [8] Krishnakkumar, R, Vignesh, N., Ramakrishnan, A., Subramanian, S., Rajesh Kana, P., "Numerical investigation on cavity fitted channel flow," In *Proceedings of the 37th national et international conference on fluid mechanics and fluid power*, Madras, Chennai, India, 2010.
- [9] Rahman, M. M., M. A. Alim, M. A. H. Mamun, M. K. Chowdhury, and A. K. M. S. Islam. "Numerical study of opposing mixed convection in a vented enclosure." *ARPJ Journal of Engineering and Applied Sciences* 2, no. 2 (2007): 25-36.
- [10] Bouaraour, K., Kholai, O., Boudebous, S., "simulation numérique de la convection mixte turbulente dans une cavité ventilée," *Algerian Journal of applied fluid mechanics* 1 (2008), ISSN, 1718-5130.
- [11] Patankar, Suhas. *Numerical heat transfer and fluid flow*. CRC press, 1980.
- [12] Doghmi, Hicham, Btissam Abourida, Lahoucine Belarache, Mohamed Sannad, and Meriem Ouzaouit. "Numerical study of mixed convection inside a three-dimensional ventilated cavity in the presence of an isothermal heating block." *INTERNATIONAL JOURNAL OF HEAT AND TECHNOLOGY* 36, no. 2 (2018): 447-456.
- [13] Jaman, Md Shah, Showmic Islam, Sumon Saha, Mohammad Nasim Hasan, and Md Quamrul Islam. "Effect of Reynolds and Grashof numbers on mixed convection inside a lid-driven square cavity filled with water-Al 2 O 3 nanofluid." In *AIP Conference Proceedings*, vol. 1754, no. 1, p. 050050. AIP Publishing, 2016.
- [14] Carozza, Antonio. "Numerical Study on Mixed Convection in Ventilated Cavities with Different Aspect Ratios." *Fluids* 3, no. 1 (2018): 11.
- [15] A. Sadikin, N. Y. Khian, Y. P. Hwey, H. Y. Al-Mahdi, I. Taib, A. N. Sadikin, S. Md Salleh, S. S. Ayop. "Effect of Number of Baffles on Flow and Pressure Drop in a Shell Side of a Shell and Tube Heat Exchangers." *Journal of Advanced Research in Fluid Mechanics and Thermal Sciences* 48, no. 2 (2018): 156-164.